

# Controllable Coupling in Phase-Coupled Flux Qubits

Mun Dae Kim

Korea Institute for Advanced Study, Seoul 130-722, Korea

We propose a scheme for tunable coupling of phase-coupled flux qubits. The phase-coupling scheme can provide a strong coupling strength of the order of Josephson coupling energy of Josephson junctions in the connecting loop, while the previously studied inductive coupling scheme cannot provide due to small mutual inductance and induced currents. We show that, in order to control the coupling, we need two dc-SQUID's in the connecting loop and the control fluxes threading the dc-SQUID's must be in opposite directions. The coupling strength is analytically calculated as a function of the control flux at the co-resonance point.

PACS numbers: 74.50.+r, 85.25.Am, 85.25.Cp

## I. INTRODUCTION

Superconducting Josephson junction qubit is one of the most promising candidates for implementing quantum computation<sup>1</sup>. Single qubit coherent oscillations in superconducting qubits have been demonstrated experimentally<sup>2,3,4</sup> and furthermore two qubit coupling and entanglement have been performed in charge<sup>5,6</sup>, flux<sup>7,8,9</sup> and phase<sup>10</sup> qubits. Scalable quantum computing requires controllable and selective coupling between two remote as well as nearest neighbor qubits. Recently much theoretical efforts have been devoted on the study about the controllable coupling of charge<sup>11</sup>, charge-phase<sup>12</sup> and flux qubits<sup>13,14,15,16</sup>. For flux qubits the controllable coupling schemes use inductive coupling, but it is too weak to perform efficient two-qubit gate operations. Hence, while in superconducting charge qubit two-qubit coherent oscillations and CNOT gate operations were experimentally observed<sup>5,6</sup>, only spectroscopy measurement was done for inductively coupled flux qubit<sup>9</sup>. In this study thus we suggest a scheme to give both strong and tunable coupling between two phase-coupled flux qubits. The phase-coupling scheme, which we previously proposed<sup>17</sup>, has been realized in a recent experiment<sup>18</sup>. The controllable coupling scheme using phase-coupled qubits with threading AC magnetic field was also studied theoretically<sup>19</sup>. Further, there have been studies about somewhat different phase-coupling schemes<sup>20,21</sup>.

Two current states of a flux qubit are characterized by the induced loop current related with the phase differences across Josephson junctions in the qubit loop. If we try to couple two flux qubits using mutual inductance, the coupling strength  $J = M I_L I_R / 0.5 \text{ GHz}^2$  will be too weak to perform the discriminating CNOT gate operations<sup>7</sup>, since the mutual inductance  $M$  and the induced currents of the left (right) qubit  $I_{L(R)}$  is very small. Even though the induced currents of flux qubits are weak, the phase differences across Josephson junctions are as large as  $\approx 2\pi$  &  $0.16$ . Hence, if two flux qubits are coupled by the phase differences between two Josephson junctions of different qubits, we can achieve a strong coupling of the order of Josephson coupling energy  $E_J^0$  of the Josephson junctions in the connecting loop whose typical

value is as large as up to about 200 GHz.

Introducing two dc-SQUID's interrupting the connecting loop as shown in Fig. 1 we can control the coupling between phase-coupled flux qubits. The control fluxes,  $f_L^0$  and  $f_R^0$ , threading two dc-SQUID loops must be in opposite directions in order to give rise to the controllable coupling. When two fluxes are in the same direction, the change of control fluxes induces an additional current flowing in the connecting loop, causing the shift of qubit states as well as the change of coupling strength. Such a dilemma also persists in the case of one dc-SQUID loop in connecting loop. However, if the control fluxes are in opposite directions, we have found that the additional currents coming from two dc-SQUID's are cancelled each other and thus the coupling strength can be tunable remaining the qubit states unchanged.

## II. PHASE-COUPLING OF FLUX QUBITS

The three-Josephson junctions qubits<sup>22,23,24</sup> in Fig. 1 has two current states; if the qubit current  $I / E_{Ji} \sin \phi_i < 0$ , it is diamagnetic while, if  $I > 0$ , paramagnetic. Introducing the notation  $j\#i$  ( $j\#i$ ) for diamagnetic (paramagnetic) current state of a qubit in pseudo spin language, there can be four current states of coupled qubits,  $j\#\#i$ ,  $j\#\#i$ ,  $j\#\#i$  and  $j\#\#i$ , of which we show one of the same current states,  $j\#\#i$ , and one of the different current states,  $j\#\#i$ , in Fig. 1. The phase  $\phi_{L1}$  and  $\phi_{R1}$  of the Josephson junctions of the three-Josephson junctions qubits have different values if two qubits are in different states. Then the phase difference  $\phi_{L1} - \phi_{R1}$  induces the phases  $\phi_i^0$  in the Josephson junctions of dc-SQUID loops.

If we neglect small kinetic inductance, the boundary conditions of the left (right) qubit and the connecting loop can be approximately written as

$$\phi_{L(R)1} + \phi_{L(R)2} + \phi_{L(R)3} = 2\pi (n_{L(R)} + f_{t;L(R)}); \quad (1)$$

$$\phi_1^0 + \phi_3^0 = 2\pi (r + f_{\text{ind}}^0) + (\phi_{L1} - \phi_{R1}); \quad (2)$$

$$\phi_1^0 + \phi_2^0 = 2\pi (f_L^0 + p); \quad \phi_3^0 + \phi_4^0 = 2\pi (f_R^0 + q); \quad (3)$$

where  $f_{t;L(R)} = f_{L(R)} + f_{\text{ind};L(R)}$  is total flux and  $f_{L(R)}^0 = 0$  with the external flux  $f_{\text{ext};L(R)}$

and the unit flux quantum  $\Phi_0 = h/2e$  is dimensionless reduced flux threading the left (right) qubit. Here  $f_{\text{ind};L(R)} = I_s L_{L(R)} / \Phi_0$  with the self inductance  $L_s$  and the induced current  $I_{L(R)}$  of qubit loop is the induced flux of each qubit and  $f_{\text{ind}}^0 = I_s^0 L^0 / \Phi_0$  that of the connecting loop and  $n_L; n_R; p$  and  $q$  are integers.

We consider that the external fluxes  $f_L$  and  $f_R$  threading the qubit loops are also in opposite directions, since they are connected in a twisted way in the scalable design of Ref. 17. However, for just two qubit coupling, we can choose the directions of external fluxes threading the qubit loops arbitrary. Actually there is no external flux in the connecting loop, but the phase difference  $(\phi_{L1} - \phi_{R1})$  in the boundary condition of Eq. (2) plays the role of effective flux in the connecting loop,

$$f_e^0 = \frac{L_1 - R_1}{2} : \quad (4)$$

When two qubits are in different current state, i.e., one is diamagnetic and the other paramagnetic, the value of  $f_e^0$  becomes 0.3-0.7. Since the induced flux of each qubit is so weak as  $f_{\text{ind}} = 0.002$ , large value of  $f_e^0 = f_{\text{ind}}$  in the phase-coupled flux qubits can give a strong coupling compared to the inductive coupling scheme.

The Hamiltonian of the coupled qubits can be given by

$$\hat{H} = \frac{1}{2} \hat{P}^T M^{-1} \hat{P} + U_e(\hat{\phi}); \quad (5)$$

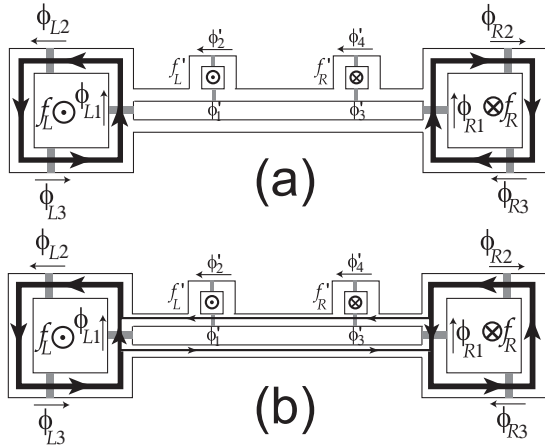


FIG. 1: Phase-coupled flux qubits with a connecting loop interrupted by two dc-SQUID's. The arrows indicate the flow of the Cooper pairs and thus in reverse direction is the current. Gray squares denote Josephson junctions with Josephson coupling energy  $E_{Ji}$  for qubit loops and  $E_J^0$  for connecting loop. The qubit operating point is  $f_L = 0.5$  and  $f_R = 0.5$ . (a) Two phase-coupled qubits are in the same current state,  $j=1$ , where two phases  $\phi_{L1}$  and  $\phi_{R1}$  are nearly equal to each other resulting negligible coupling energy. Here  $j=1$  and  $j=2$  denote the diamagnetic and paramagnetic current state, respectively. (b) Left (right) qubit is in the diamagnetic (paramagnetic) current state,  $j=1$ , where the large phase difference,  $\phi_{L1} - \phi_{R1}$ , induces large Josephson energy and current in the connecting loop.

which describes dynamics of a particle with effective mass  $M$  in the effective potential  $U_e(\hat{\phi})$  with  $\hat{\phi} = (\phi_{L1}; \phi_{L2}; \phi_{L3}; \phi_{R1}; \phi_{R2}; \phi_{R3}; \phi_0; \phi_0; \phi_0; \phi_0)$ . The kinetic part of the Hamiltonian comes from the charging energy of the Josephson junctions such as

$$E_C(\hat{\phi}) = \frac{1}{2} \sum_{P=L;R} \sum_{i=1}^3 \frac{Q_i^2}{C_P} + C_P^0 \frac{\phi_P^2}{2} ; \quad (6)$$

where  $C_{L(R)i}$  and  $C^0$  is the capacitance of the Josephson junctions of the left (right) qubit loop and the connecting loop, respectively. The number of excess Cooper pair charges on Josephson junction  $\hat{N}_i = \hat{Q}_i / q_c$  is conjugate to the phase difference  $\hat{\phi}_i$  such as  $[\hat{\phi}_i; \hat{N}_i] = i$ , where  $Q_i = C_i (\phi_0 = 2\pi) / q_c$ ,  $q_c = 2e$  and  $C_i$  the capacitance of the Josephson junctions. Here we introduce the canonical momentum  $\hat{P}_i$  and the effective mass  $M_{ij}$

$$\hat{P}_i = \hat{N}_i \sim -i \frac{\partial}{\partial \hat{\phi}_i}; \quad M_{ij} = \frac{1}{2} \frac{\partial^2}{\partial \hat{\phi}_i \partial \hat{\phi}_j} C_{ij}; \quad (7)$$

to obtain the kinetic part of the Hamiltonian.

The effective potential of the coupled qubits is composed of the inductive energy of loops and the Josephson junction energy terms;

$$U_e(\hat{\phi}) = U_{\text{ind}}(\hat{\phi}) + U_{\text{qubit}}(\hat{\phi}) + U_{\text{conn}}(\hat{\phi}); \quad (8)$$

$$U_{\text{ind}}(\hat{\phi}) = \frac{1}{2} L_s (I_L^2 + I_R^2) + \frac{1}{2} L_0 I_0^2 \quad (9)$$

$$U_{\text{qubit}}(\hat{\phi}) = \sum_{i=1}^3 E_{Ji} (1 - \cos \phi_{Li}) + \sum_{i=1}^3 E_{Ji} (1 - \cos \phi_{Ri}) \quad (10)$$

$$U_{\text{conn}}(\hat{\phi}) = \sum_{i=1}^3 E_J^0 (1 - \cos \phi_i) ; \quad (11)$$

Here  $U_{\text{ind}}(\hat{\phi})$  is the inductive energy of loops with the current of the right qubit  $I_R$ , left qubit  $I_L$  and connecting loop  $I_0$ .  $U_{\text{qubit}}(\hat{\phi})$  is the energy of the Josephson junctions in two qubit loop and  $U_{\text{conn}}(\hat{\phi})$  that of the connecting loop with Josephson coupling energies  $E_{Ji}$  and  $E_J^0$ .

In experiments the two Josephson junctions with phase differences  $\phi_{L(R)2}$  and  $\phi_{L(R)3}$  can be considered nominally the same so that it is reasonable to set

$$E_{J2} = E_{J3} = E_J; \quad \phi_{L(R)2} = \phi_{L(R)3}; \quad (12)$$

Here we introduce a rotated coordinate

$$p = (\phi_{L3} + \phi_{R3}) / 2; \quad (13)$$

$$m = (\phi_{L3} - \phi_{R3}) / 2 \quad (14)$$

and then using the boundary conditions in Eq. (1) we get

$$\phi_{L1} - \phi_{R1} = 4 p^{(m)} + 2 (n_L \phi_{L2} - n_R \phi_{R2} + f_L \phi_L - f_R \phi_R); \quad (15)$$

Thus we can reexpress the sum of Josephson junction energies of both qubits as

$$U_{\text{qubit}}(\phi_m, \phi_p) = 2E_{J1} [1 - \cos(P\phi_p - 2\phi_m)] \cos(M\phi_m) + 4E_J (1 - \cos\phi_p \cos\phi_m); \quad (16)$$

where  $P = n_L + n_R + f_L + f_R + f_{\text{ind};L} + f_{\text{ind};R}$  and  $M = n_L - n_R + f_L - f_R + f_{\text{ind};L} - f_{\text{ind};R}$ . Since experimentally qubit operations are performed at near the co-resonance point  $f_L = f_R = 0.5$  and the induced flux is so weak as  $f_{\text{ind};L(R)} \approx 0.002$ ,  $P$  and  $M$  can be approximated as integers such that  $P = n_L + n_R + 1$  and  $M = n_L - n_R$ . If  $P$  is even,  $M$  is odd and vice versa, so we can get simple form for  $U_{\text{qubit}}(\phi_m, \phi_p)$ ,

$$U_{\text{qubit}}(\phi_m; \phi_p) = 2E_{J1} \cos 2\phi_p \cos 2\phi_m + 4E_J \cos\phi_p \cos\phi_m + 2E_{J1} + 4E_J; \quad (17)$$

Introducing another rotated coordinate

$$\phi_p^0 = \begin{pmatrix} \phi_p \\ \phi_m \end{pmatrix} = 2; \quad (18)$$

$$\phi_m^0 = \begin{pmatrix} \phi_p \\ \phi_m \end{pmatrix} = 2 \quad (19)$$

and using the boundary conditions in Eq. (3) to get

$$\begin{pmatrix} \phi_p^0 \\ \phi_m^0 \end{pmatrix} = 2 = \begin{pmatrix} \phi_p^0 \\ \phi_m^0 \end{pmatrix} + (f_L^0 - f_R^0 + p - q); \quad (20)$$

the Josephson junction energy of the connecting loop  $U_{\text{conn}}(\phi_m^0) = \sum_{i=1}^4 E_J^0 (1 - \cos\phi_i^0)$  can also be written as

$$U_{\text{conn}}(\phi_m^0; \phi_p^0) = 2E_J^0 = 2 \cos\phi_m^0 \cos\phi_p^0 \cos[\phi_m^0 + (f_L^0 + f_R^0)] \cos[\phi_p^0 + (f_L^0 - f_R^0)]; \quad (21)$$

where we set  $p = 0$  and  $q = 0$ .

### III. COUPLED QUBIT STATES IN EFFECTIVE POTENTIAL

First of all we consider the case that the control fluxes,  $f_L^0$  and  $f_R^0$ , have opposite directions such that

$$f_L^0 = f_R^0 = f^0; \quad (22)$$

Note that the boundary conditions in Eq. (3) already have opposite signs. In order to obtain the effective potential as a function of  $\phi_m$  and  $\phi_p$ , we reexpress  $\phi_p^0$  as  $\phi_p^0 = (f_e^0 + r + f_{\text{ind}}^0) = 2\phi_m + M^0$  using the boundary conditions in Eq. (2) and the expression in Eq. (15). Here  $M^0 = M + r + f_{\text{ind}}^0$  can be written as  $M^0 = n_L - n_R + r$  neglecting small induced flux  $f_{\text{ind}}^0$  in the connecting loop. Depending on whether  $M^0$  is even or odd, the results will be quantitatively different, but qualitatively the same. Here and after, thus, we choose  $M^0$  is even and specially  $n_L = 0$ ,  $n_R = 0$  and  $r = 0$  for simplicity and then  $\phi_p^0$  becomes

$$\phi_p^0 = f_e^0 = 2\phi_m; \quad (23)$$

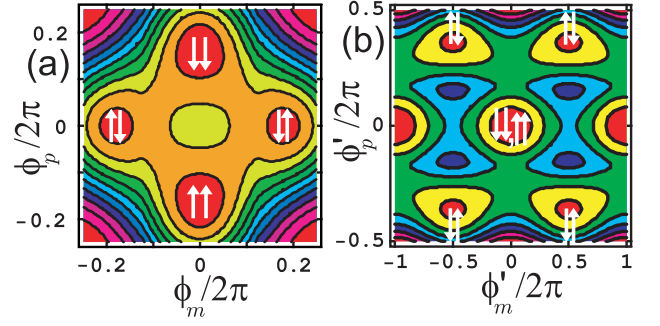


FIG. 2: (Color online) Effective potential of the coupled qubits in Eq. (25) for  $E_J^0 = 0.1E_J$  when  $f_L^0 = f_R^0 = f^0 = 0$  (a) in  $(\phi_m^0; \phi_p^0)$  plane and (b) in  $(\phi_m^0; \phi_p^0)$  plane. Coupled qubit states at the local minima of potentials are denoted in pseudospin notation, which shows that these states are stable in both planes. Here we set  $E_{J1} = E_J$  and  $f_L = f_R = 0.5$ .

and the energy of Josephson junctions in connecting loop in Eq. (21)

$$U_{\text{conn}}(\phi_m^0; \phi_p^0) = 4E_J^0 [1 - \cos f^0 \cos(\phi_m^0 + f^0) \cos 2\phi_m]; \quad (24)$$

Since the induced energy  $U_{\text{ind}}(\phi)$  can be negligible, the total effective potential  $U_e(\phi)$  in Eq. (8) is given by the sum of the energies in Eqs. (17) and (24),

$$U_e(\phi_m; \phi_p; \phi_m^0) = U_{\text{qubit}}(\phi_m; \phi_p) + U_{\text{conn}}(\phi_m^0; \phi_p^0); \quad (25)$$

The lowest energy level of  $U_e$  in  $(\phi_m; \phi_p)$  plane can be obtained by setting the remaining variable  $\phi_m^0$  in Eq. (24) as

$$(i) \quad \phi_m^0 = 0; \quad \text{for } -4 < \phi_m < 4; \quad (26)$$

$$(ii) \quad \phi_m^0 = \pi; \quad \text{for } -4 < \phi_m < -2; \quad (27)$$

when  $f^0 = 0$ . We plot the effective potential  $U_e(\phi_m; \phi_p)$  in Fig. 2 (a) with four local minima.

The value of local minima of case (i) can be obtained from  $U_e(\phi_m = 0; \phi_p)$  and we have found that two local minima have the same value,  $E_{ss}(f^0)$ , for equal pseudospin state with  $s = \pm f^0$ . Similarly we get  $E_{s; s}(f^0)$  of case (ii) from  $U_e(\phi_m; \phi_p = 0)$  for different pseudospin state. As a result, we obtain

$$E_{ss^0}(f^0) = 4E_J + 4E_J^0 (1 - \cos f^0) + 2E_J \cos ss^0; \quad (28)$$

where  $ss$  is the value of  $\phi_p$  at local minima of the same spin states,  $jsi$ , and  $s; s$  the value of  $\phi_m$  of the different spin states,  $js; si$  with

$$\cos ss = \frac{E_J}{2E_{J1}}; \quad (29)$$

$$\cos s; s = \frac{E_J}{2(E_{J1} + 2E_J^0 \cos f^0)}; \quad (30)$$

Thus the energy of the same spin states,  $E_{ss}(f^0 = 0)$ , is lower than that of different spin states,  $E_{s; s}(f^0 = 0)$ , as shown in Fig. 2 (a).

Here we set  $E_{J1} = E_J$ ,  $E_J^0 = 0.1E_J$  and  $f_L = f_R = 0.5$ . For the same spin states we have two solutions,  $\phi_{ss=2} = \phi_{1=6}$ , corresponding to two local minima,  $E_{\#\#}(f^0 = 0)$  and  $E_{\#\#\#}(f^0 = 0)$ . When  $\phi_{ss=2} = \phi_{1=6}$ ,  $\phi_{p=2} = \phi_{1=6}$  and  $\phi_m = 0$  and thus

$$\phi_{L(R)2=2} = \phi_{L(R)3=2} = \phi_{L(R)1=2} = \phi_{1=6} \quad (31)$$

using  $\phi_{L(R)1} + 2\phi_{L(R)3} = \phi_{1=6}$  from the boundary condition in Eq. (1) with  $n_{L(R)} = 0$ . Since the loop currents of both qubits then

$$I = (2 = 0)E_J \sin \phi_{L(R)3}; \quad (32)$$

are diamagnetic as can be seen from Fig. 1(a), this coupled-qubits state can be represented as  $j\#\#i$  as shown in Fig. 2 (a). On the other hand, when  $\phi_{ss=2} = \phi_{1=6}$ ,

$$\phi_{L(R)2=2} = \phi_{L(R)3=2} = \phi_{1=6}; \quad \phi_{L(R)1=2} = \phi_{5=6}; \quad (33)$$

Then the qubit current  $I = (2 = 0)E_J \sin(\phi_{=3}) = (2 = 0)E_J \sin(\phi_{5=3})$  corresponds to the paramagnetic current states,  $j\#\#\#i$ . We would like to note that, since the external fluxes  $\phi_L$  and  $\phi_R$  threading left and right qubit loops are already in opposite directions, diamagnetic (paramagnetic) currents of both qubits in  $j\#\#i$  ( $j\#\#\#i$ ) state are also in opposite directions.

For different spin states, two solutions are also obtained for  $\phi_{s; s=2} = 0.181$ . When  $\phi_{s; s=2} = 0.181$ ,

$$\phi_{L2=2} = \phi_{L3=2} = 0.181; \quad \phi_{L1=2} = 0.138 \quad (34)$$

$$\phi_{R2=2} = \phi_{R3=2} = 0.181; \quad \phi_{R1=2} = 0.862 \quad (35)$$

for left and right qubit respectively, which corresponds to the state,  $j\#\#i$  in Fig. 2 (a). In the same way  $\phi_{s; s=2} = 0.181$  corresponds to the state  $j\#\#i$ . Hence we can identify four stable states,  $j\#\#i; j\#\#\#i; j\#\#i$  and  $j\#\#i$ , with energies  $E_{ss}$  and  $E_{s; s}$  at the local minima of  $U_e(\phi_m; \phi_p)$  as shown in Fig. 2 (a).

Even though above four states are stable states in  $(\phi_m; \phi_p)$  plane, it can be unstable in the other dimensions if they are saddle points. Thus we need represent the effective potential  $U_e$  in  $(\phi_m^0; \phi_p^0)$  plane. From the

$jss^0i$	$(\phi_{R3=2}; \phi_{L3=2})$	$(\phi_m=2; \phi_p=2)$	$(\phi_m^0=2; \phi_p^0=2)$
$j\#\#i$	(1/6, 1/6)	(0; 1=6)	(0, 0)
$j\#\#\#i$	(1=6; 1=6)	(0; 1=6)	(0, 0)
$j\#\#i$	(0.181; 0.181)	(0.181; 0)	(0.5; 0.362)
$j\#\#i$	(0.181; 0.181)	(0.181; 0)	(0.5; 0.362)

TABLE I: The values of phase differences of coupled qubits states in several coordinates with  $E_{J1} = E_J$ ,  $E_J^0 = 0.1E_J$ ,  $f_L = f_R = 0.5$  and  $f^0 = 0$ .

expression of  $U_e(\phi_m; \phi_p; \phi_m^0)$  in Eq. (25) and the relation  $\phi_p^0 = 2\phi_m$  in Eq. (23), we can get  $U_e(\phi_m^0; \phi_p^0; \phi_p)$  and, following similar procedure as in the  $(\phi_m; \phi_p)$  plane, we obtain the effective potential as shown in Fig. 2 (b), where we can again see local minima. In Figs. 2 (b), for the states  $j\#\#i$  and  $j\#\#\#i$  of case (i), we can get the values

$$\phi_p^0 = 0 \text{ and } \phi_m^0 = 0; \quad (36)$$

and, for case (ii), the values

$$\begin{aligned} \phi_p^0=2 &= 0.362; \quad \phi_m^0=2 = 0.5; \text{ for } j\#\#\#i \\ \phi_p^0=2 &= 0.362; \quad \phi_m^0=2 = 0.5; \text{ for } j\#\#i \end{aligned} \quad (37)$$

using Eqs. (23), (26) and (27) and the values of  $\phi_m$  in each case. As a result, we are able to identify the spin states at local minima of Figs. 2 (b) from Fig. 2 (a) with above values and confirm the stability of the states in both planes. In Table I we summarize the values of the phase differences for four states,  $jss^0i$ , of coupled qubits in several coordinates. Actually we obtained higher energy states in Fig. 2 (a), but found that they are unstable in  $(\phi_m^0; \phi_p^0)$  plane.

#### IV. TUNABLE COUPLING OF FLUX QUBITS

The Hamiltonian of coupled qubits can be written as

$$\begin{aligned} H_{\text{coup}} &= h_L \frac{z}{L} I + h_R I \frac{z}{R} + J \frac{z}{L} \frac{z}{R} \\ &+ t_L \frac{x}{L} I + t_R I \frac{x}{R} + E_0; \end{aligned} \quad (38)$$

where  $h_L = (E_{\#\#} + E_{\#\#\#})/2 = E_0$  and  $h_R = (E_{\#\#} + E_{\#\#\#})/2 = E_0$  with  $E_0 = (E_{\#\#} + E_{\#\#\#} + E_{\#\#} + E_{\#\#\#})/4$  and  $I$  is the  $2 \times 2$  identity matrix. First two terms are qubit terms, the third is coupling term and last two terms are tunnelling terms which come from the quantum fluctuation described by the kinetic term of the Hamiltonian. Then the coupling constant  $J$  of the coupled qubits is given by<sup>17</sup>

$$J = \frac{1}{4} (E_{\#\#\#} + E_{\#\#} - E_{\#\#} - E_{\#\#\#}); \quad (39)$$

In Fig. 3 we plot the energies of coupled-qubits for various  $f^0$  with  $E_J^0 = 0.1E_J$ ,  $E_{J1} = E_J$  and  $f_L = f_R = 0.5$  in  $(\phi_{R3}; \phi_{L3})$  plane. When  $f^0 = 0$  in Fig. 3(a), the energies  $E_{ss}$  of the same spin states,  $j\#\#i$  and  $j\#\#\#i$ , are lower than  $E_{s; s}$ , of the different spin states,  $j\#\#i$  and  $j\#\#\#i$ . The positions of four local minima are shown in Table I. As  $f^0$  increases, the energy difference  $E = E_{s; s} - E_{ss}$  becomes smaller (upper panel in (b)) and finally  $E = 0$  at  $f^0 = 0.5$  in (c). Since  $E_{\#\#\#} = E_{\#\#} = E_{ss}$  and  $E_{\#\#} = E_{\#\#\#} = E_{s; s}$ , the coupling strength can be written as

$$2J(f^0) = E(f^0) = E_{s; s}(f^0) - E_{ss}(f^0); \quad (40)$$

Therefore the coupling strength between two flux qubits changes as varying the control flux  $f^0$  threading the dc-SQUID loop in the connecting loop.

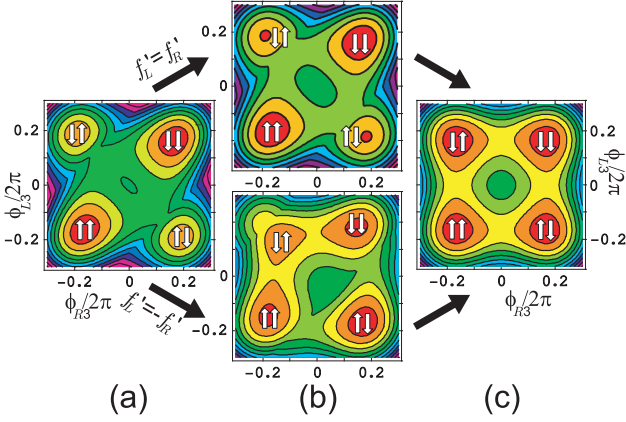


FIG. 3: (Color online) E effective potential of the coupled qubits in Eq. (8) for  $E_J^0 = 0.1E_J$ ,  $E_{J1} = E_J$  and  $f_L = f_R = 0.5$ . Coupled qubit states at the local minima of potentials are denoted in pseudo-spin notation. (a) E effective potential as a function of  $\phi_{R3}$  and  $\phi_{L3}$  when  $f_L^0 = f_R^0 = f^0 = 0$  for the phase-coupled qubits in Fig. 1. Here the energies of different current states are equal to each other,  $E_{\# \#} = E_{\# \#}$ , as well as  $E_{\# \#} = E_{\# \#}$  for the same current states. The energy of different current states  $E_{s; s} = E_{\# \#} = E_{\# \#}$  is higher than that of the same current states  $E_{ss} = E_{\# \#} = E_{\# \#}$ . (b) (top) Two control axes in Fig. 1 are in opposite directions,  $f_L^0 = f_R^0 = f^0$ , and  $f^0$  is increased to  $f^0 = 0.25$ . The energy difference  $E = E_{s; s} - E_{ss}$  becomes smaller than when  $f^0 = 0$  in (a). (bottom) For the case when two control axes are in the same direction such as  $f_L^0 = f_R^0 = f^0 = 0.25$ , the energies of different current states are not equal to each other anymore;  $E_{\# \#} > E_{\# \#}$ . (c) The coupling becomes switched on when  $f_L^0 = f_R^0 = f^0 = 0.5$ . Thus the energies of four states have the same value,  $E_{\# \#} = E_{\# \#} = E_{\# \#} = E_{\# \#}$ .

From Eq. (28) the coupling constant  $J$  can be represented as a function of  $f^0$  by  $J(f^0) = E_J \cos_{ss} \cos_{s; s}$ , which gives

$$J(f^0) = \frac{E_J^2 \cos f^0}{E_{J1} E_{J1} + 2E_J^0 \cos f^0}; \quad (41)$$

In Fig. 4 (a) we plot the energies  $E_{ss^0}(f^0)$  and  $J(f^0)$  as a function of  $f^0$ , where  $2J(f^0) = E_{s; s}(f^0) - E_{ss}(f^0)$ . When  $f^0 = 0$ ,  $J$  is of the order of  $E_J^0$  so that we can obtain a sufficiently strong coupling. By adjusting  $f^0$  the coupling strength can be tuned from strong coupling to zero at  $f^0 = 0.5$ .

The coupling strength  $J(f^0)$  in Eq. (41) depends on  $E_J = E_{J1}$  as well as  $E_J^0$ . When  $E_J^0 = E_{J1}$  is small,  $J(f^0)$  is proportional to  $E_J^0$  and  $(E_J = E_{J1})^2$ . Recently the phase-coupling scheme has been experimentally implemented<sup>18</sup>, where four-Josephson junction qubits are employed instead of usual three-Josephson junction qubits. In that experiment the Josephson junction energy  $E_{J1}$  of fourth junction is large so that the value of  $E_J = E_{J1}$  is about  $E_J = E_{J1} = 3$ . As a result, the experiment exhibits rather small coupling strength.

The current of connecting loop can be written as

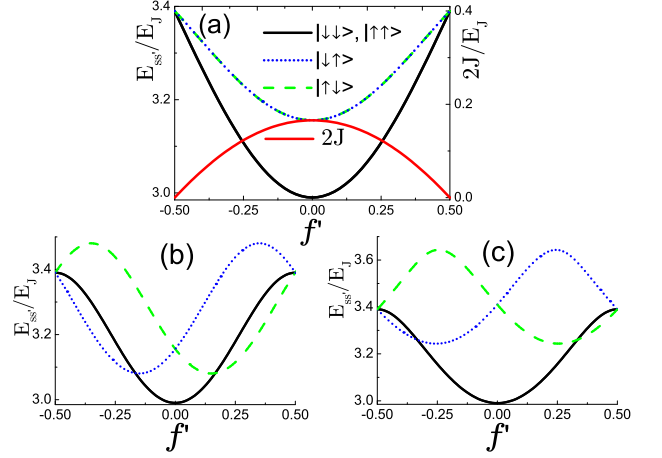


FIG. 4: (Color online) Energies of coupled qubit states for  $E_J^0 = 0.1E_J$ ,  $E_{J1} = E_J$  and  $f_L = f_R = 0.5$  as a function of  $f^0$ . (a)  $E_{ss^0}(f^0)$  in Eq. (28) when two control axes in Fig. 1 are in opposite directions,  $f_L^0 = f_R^0 = f^0$ . The coupled qubits can be described by the Hamiltonian in Eq. (38) and the coupling strength  $2J(f^0) = E_{s; s}(f^0) - E_{ss}(f^0)$  in Eq. (41) is also shown. As  $f^0$  increases, the coupling strength decreases monotonously, vanishing finally at  $f^0 = 0.5$ . (b) When two control axes in Fig. 1 are in the same direction,  $f_L^0 = f_R^0 = f^0$ , the energy of two states,  $|j\#\#i$  and  $|j\#i$ , becomes different, as if additional axes,  $f_L$  and  $f_R$ , were applied into the left and right qubit loop, respectively. Hence the coupling between two qubits cannot be represented solely by change of the coupling constant of the Hamiltonian in Eq. (38). (c) For the case when there is only one dc-SQUID loop in the connecting loop instead of two dc-SQUID's in Fig. 1, the energies of the different current states,  $|j\#\#i$  and  $|j\#i$ , are also different from each other.

$(\sum_{i=1}^2)I^0 = E_J^0 \sum_{i=1}^2 \sin \phi_i = E_J^0 \sum_{i=3}^4 \sin \phi_i$ , which gives the relations,  $(\begin{smallmatrix} 0 & 1 \\ 1 & 0 \end{smallmatrix}) + (\begin{smallmatrix} 0 & 2 \\ 2 & 0 \end{smallmatrix}) = 4k$  and then

$$I_m^0 = (k - f^0); \quad (42)$$

with integer  $k$  using the boundary conditions in Eq. (3). Then, using Eq. (20) and the effective flux  $\Phi_e^0$  in Eq. (23), the current  $(\sum_{i=1}^2)I^0 = 0.5E_J^0 \sum_{i=1}^4 \sin \phi_i$  is given by

$$I^0 = \frac{2}{\phi_e^0} (\sum_{i=1}^4) 2E_J^0 \cos f^0 \sin \phi_e^0; \quad (43)$$

This current-phase relation can be considered as the Josephson junction type relation,  $I^0 = (\sum_{i=1}^4) E_J^0 \sin \phi'$ , with the effective Josephson coupling energy,  $E_J^0$ , of two dc-SQUID's in the connecting loop

$$E_J^0 = 2E_J^0 \cos f^0 \quad (44)$$

and the phase difference  $\phi' = \phi_e^0$ . The coupling constant in Eq. (41) also can be represented by the effective Josephson coupling energy,  $E_J^0$ . Thus the large phase difference,  $\phi_e^0$ , and the Josephson coupling energy,  $E_J^0$ ,

induce the current in the connecting loop and the coupling energy of the phase-coupled qubits.

For the same spin states,  $j_{\#}^{\uparrow}$  and  $j_{\#}^{\downarrow}$ , the current of connecting loop  $I^0$  becomes zero, since  $I_L = I_R$  and thus  $f_e^0 = 0$ . For a different spin states  $j_{\#}^{\uparrow}$  with  $f^0 = 0$ ,  $f_e^0 = (I_L - I_R)/2 = 0.724$  and we have  $k = 1$  from  $\cos \theta_m = 1$  and the relation in Eq. (42). Then weak current  $I^0$  in the connecting loop flows satisfying current conservation condition between left qubit and connecting loop such that  $E_J \sin 0.181(2) = E_{J1} \sin 0.138(2) + 2E_J^0 \sin 0.724$  for  $f^0 = 0$ . When  $f^0$  approaches 0.5, the effective Josephson coupling energy  $E_J^0 = E_J \cos f^0$  and thus the current  $I^0$  in connecting loop become zero, which means that the coupling between two qubits is switched off.

Now we want to explain the case that two control fluxes are in the same directions and the case that there is only single dc-SQUID in connecting loop. If two control fluxes are in the same direction such as

$$f_L^0 = f_R^0 = f^0; \quad (45)$$

the Josephson junction energy of the connecting loop becomes

$$U_{\text{conn}}(\theta_m; \theta) = 4E_J^0 [1 - \cos f^0 \cos \theta_m \cos(2\theta_m - f^0)]; \quad (46)$$

Similar procedure as in the case of opposite directions of control fluxes shows that the same spin states,  $j_{\#}^{\uparrow}$  and  $j_{\#}^{\downarrow}$ , have equal energy such as

$$E_{\#}^{\uparrow} = E_{\#}^{\downarrow} = E_J \left[ 4 \frac{E_J}{E_{J1}} + 4E_J^0 \sin^2 f^0 \right]; \quad (47)$$

for  $\cos \theta_p = E_J = 2E_{J1}$ .

For different spin states,  $j_{\#}^{\uparrow}$  and  $j_{\#}^{\downarrow}$ , the energies  $E_{\#}^{\uparrow}$  and  $E_{\#}^{\downarrow}$  are obtained at two local minima

$$U_{\text{conn}}(\theta_m; \theta_p = 0) = 4E_J^0 \cos^2 f^0 \cos 2\theta_m - 2E_J^0 \sin 2f^0 \sin 2\theta_m + 4E_J^0; \quad (48)$$

which can be derived from Eq. (46). Since the states,  $j_{\#}^{\uparrow}$  and  $j_{\#}^{\downarrow}$ , have different sign for  $s_j$ ,  $s_j$ , the second term produces the energy difference

$$E = E_{\#}^{\uparrow} - E_{\#}^{\downarrow} = 4E_J^0 \sin 2f^0 j \sin 2s_j; \quad (49)$$

where  $s_j$ ,  $s_j$  is again one of the values of  $\theta_m$  for the different spin states.

Figure 3(b) (lower panel) for  $f^0 = 0.25$  shows that, when two control fluxes are in the same direction, the energies  $E_{\#}^{\uparrow}$  and  $E_{\#}^{\downarrow}$  are different while  $E_{\#}^{\uparrow} = E_{\#}^{\downarrow}$ . The energy levels of  $E_{ss^0}$  are plotted in Fig. 4(b). In this case the effective fluxes  $h_L$  and  $h_R$  applied to left and right qubits in the Hamiltonian of Eq. (38) become different each other,  $h_L \neq h_R$ , as  $f^0$  increases from zero. For the different current state in Fig. 1(b), if the control fluxes  $f_L^0$  and  $f_R^0$  threading the dc-SQUID loops are in the

same direction, the increased current  $I^0$  in the connecting loop will flow through the left and right qubit loops. Thus the qubit states are influenced by additional effective fluxes, which will make the two-qubit operations difficult. However, if two control fluxes  $f_L^0$  and  $f_R^0$  are in opposite directions, the energies of different spin states remain equal to each other,  $E_{\#}^{\uparrow} = E_{\#}^{\downarrow}$ , as shown in Fig. 4(a). This means that the additional currents coming from two dc-SQUID's are cancelled each other and total additional current induced by the control fluxes  $f_L^0$  and  $f_R^0$  is vanishing in the connecting loop. As a result, the net effect is just renormalizing the coupling constant  $J$  of the coupled qubit system.

We also calculated energies of coupled qubit states with single dc-SQUID loop whose boundary conditions become

$$\psi_1^0 = 2(\alpha + f_{\text{ind}}^0) + (I_L - I_R) \quad (50)$$

$$\psi_1^0 + \psi_2^0 = 2(f^0 + p); \quad (51)$$

instead of those in Eqs. (2) and (3). Then we get the Josephson junction energies of the dc-SQUID,

$$U_{\text{conn}}(\theta_m) = 2E_J^0 \cos(4\theta_m - f^0) + 2E_J^0; \quad (52)$$

which gives results similar to those of two dc-SQUID's with fluxes in the same direction such that

$$E_{\#}^{\uparrow} = E_{\#}^{\downarrow} = E_J \left[ 4 \frac{E_J}{E_{J1}} + 2E_J^0 \sin^2 f^0 \right] \quad (53)$$

for  $\cos \theta_p = E_J = 2E_{J1}$  and

$$E = E_{\#}^{\uparrow} - E_{\#}^{\downarrow} = 2E_J^0 \sin 2f^0 j \sin 4s_j; \quad (54)$$

as shown in Fig. 4(c). Hence the behaviors of one dc-SQUID in the connecting loop are qualitatively the same as those of two dc-SQUID's with fluxes in the same direction. Therefore we need two control fluxes threading dc-SQUID's in opposite directions to cancel the additional currents in the connecting loop for obtaining the controllable coupling.

In order to obtain the controllable coupling both the qubit operating flux,  $f_L$ , and control flux,  $f_L^0$ , of the left qubit become in opposite direction to those of the right qubit,  $f_R$  and  $f_R^0$  as shown in Fig. 1. In real experiments it will be very hard to apply magnetic fluxes of different directions simultaneously. We have previously suggested a scalable design for phase-coupled flux qubits<sup>7</sup>, where an arbitrary pair of qubits are coupled in a twisted way. Thus just applying all magnetic fluxes in the same direction makes automatically the effect of fluxes in opposite directions, removing the experimental difficulty.

The recent experiment on the phase-coupled flux qubits without dc-SQUID loop<sup>18</sup> has shown that the coupled qubit states are in quantum mechanically superposed regime. The dc-SQUID loops in the connecting loop of the present tunable coupling scheme may cause a decoherence effect on the coupled qubit states. A recent study argued that the dc-SQUID based oscillator

should be the main source of the decoherence of the qubits<sup>25</sup>. For the scalable design in Ref. 17, however, the decoherence from two dc-SQUID's can be reduced. Since two dc-SQUID's are connected in a twisted way, the fluctuations from tank circuit or flux lines can be cancelled each other.

In realistic implementation of qubit operations, operating external fluxes are slightly different from the co-resonance point,  $f_L = f_R = 0.5$ , and moreover we cannot any more neglect small kinetic inductance and induced fluxes. Hence we confirmed the results in this study by numerical calculation using the exact boundary conditions similar to those in Eqs. (1)–(3), current-phase relation  $I_i = (2e_0)E_{J_i} \sin \phi_i$  and current conservation conditions<sup>17</sup>.

## V. SUMMARY

Controllable coupling between two phase-coupled flux qubits can be achieved by using two dc-SQUID's in the

connecting loop with threading fluxes in opposite directions. We analytically show at co-resonance point ( $f_L = f_R = 0.5$ ) that the coupling strength of the phase-coupled flux qubits can be adjusted by varying the threading fluxes<sup>2</sup> from 0 to 0.5; it can be as strong as  $O(E_J^0)$  and zero in switching-on limit. When either two control fluxes are in the same directions or there is only one dc-SQUID in the connecting loop, the coupled qubits cannot be described by the coupling Hamiltonian. In slightly different parameter regimes of experimental implementations numerical calculations can be done to obtain exact results.

## ACKNOWLEDGMENTS

This work was supported by the Ministry of Science and Technology of Korea (Quantum Information Science).

- 
- <sup>1</sup> Y. Makhlin, G. Schon, and A. Shnirman, *Rev. Mod. Phys.* **73**, 357 (2001); A. Galindo and M. A. Martin-Delgado, *ibid.* **74**, 347 (2002).
  - <sup>2</sup> Y. Nakamura, Yu. A. Pashkin, and J. S. Tsai, *Nature* **398**, 786 (1999).
  - <sup>3</sup> Y. Yu, S. Han, X. Chu, S. Chu, and Z. Wang, *Science* **296**, 889 (2002).
  - <sup>4</sup> I. Chiorescu, Y. Nakamura, C. J. P. M. Hamans, and J. E. Mooij, *Science* **299**, 1869 (2003).
  - <sup>5</sup> Yu. A. Pashkin, T. Yamamoto, O. Astaev, Y. Nakamura, D. V. Averin, and J. S. Tsai, *Nature* **421**, 823 (2003).
  - <sup>6</sup> T. Yamamoto, Yu. A. Pashkin, O. Astaev, Y. Nakamura, and J. S. Tsai, *Nature* **425**, 941 (2003).
  - <sup>7</sup> A. Izmailkov, M. G. Rajar, E. Ilchev, Th. Wagner, H.-G. Meyer, A. Yu. Smirnov, M. H. S. Amin, A. Lec M aassen van den Brink, and A. M. Zagoskin, *Phys. Rev. Lett.* **93**, 037003 (2004).
  - <sup>8</sup> M. G. Rajar, A. Izmailkov, S. H. W. van der Ploeg, S. Linzen, E. Ilchev, Th. Wagner, U. Hubner, H.-G. Meyer, A. Lec M aassen van den Brink, S. Uchaikin, and A. M. Zagoskin, *Phys. Rev. B* **72**, 020503(R) (2005).
  - <sup>9</sup> J. B. Majer, F. G. Paauw, A. C. J. ter Haar, C. J. P. M. Hamans, and J. E. Mooij, *Phys. Rev. Lett.* **94**, 090501 (2005).
  - <sup>10</sup> A. J. Berkley et al., *Science* **300**, 1548 (2003).
  - <sup>11</sup> D. V. Averin and C. Bruder, *Phys. Rev. Lett.* **91**, 057003 (2003); J. Q. You, J. S. Tsai, and F. Nori, *Phys. Rev. B* **68**, 024510 (2003).
  - <sup>12</sup> A. Blais, A. Lec M aassen van den Brink, and A. M. Zagoskin, *Phys. Rev. Lett.* **90**, 127901 (2003).
  - <sup>13</sup> B. L. T. Plurde et al., *Phys. Rev. B* **70**, 140501(R) (2004).
  - <sup>14</sup> P. Bertet, C. J. P. M. Hamans, and J. E. Mooij, *Phys. Rev. B* **73**, 064512 (2006).
  - <sup>15</sup> Y.-x. Liu, L. F. Wei, J. S. Tsai, and F. Nori, *Phys. Rev. Lett.* **96**, 067003 (2006).
  - <sup>16</sup> A. O. Niskanen, Y. Nakamura, and J. S. Tsai, *Phys. Rev. B* **73**, 094506 (2006).
  - <sup>17</sup> M. D. Kin and J. Hong, *Phys. Rev. B* **70**, 184525 (2004).
  - <sup>18</sup> S. H. W. van der Ploeg, A. Izmailkov, A. Lec M aassen van den Brink, U. Hubner, M. G. Rajar, E. Ilchev, H.-G. Meyer, and A. M. Zagoskin, *cond-mat/0605588*.
  - <sup>19</sup> M. G. Rajar, Y.-x. Liu, F. Nori, and A. M. Zagoskin, *cond-mat/0605484*.
  - <sup>20</sup> M. G. Rajar et al., *Phys. Rev. Lett.* **96**, 047006 (2006).
  - <sup>21</sup> A. Lec M aassen van den Brink, *cond-mat/0605398*.
  - <sup>22</sup> J. E. Mooij et al., *Science* **285**, 1036 (1999); Caspar H. van der Wal et al., *Science* **290**, 773 (2000).
  - <sup>23</sup> T. P. Orlando et al., *Phys. Rev. B* **60**, 15398 (1999).
  - <sup>24</sup> M. D. Kin, D. Shin, and J. Hong, *Phys. Rev. B* **68**, 134513 (2003).
  - <sup>25</sup> P. Bertet, I. Chiorescu, G. Burkard, K. Semba, C. J. P. M. Hamans, D. P. Di Vincenzo, and J. E. Mooij, *Phys. Rev. Lett.* **95**, 257002 (2005).